11176-H546-RO-00

PROJECT TECHNICAL REPORT

TASK E-9G

COMMUNICATIONS STUDY FOR THE PARTICLES AND FIELDS LUNAR SUBSATELLITE

NAS 9-8166

21 May 1970

Prepared for

NATIONAL AERONAUTICS AND SPACE ADMINISTRATION
MANNED SPACECRAFT CENTER
HOUSTON, TEXAS



Prepared by


Communication and Sensor Systems Department
Electronics Systems Laboratory


TRW
SYSTEMS GROUP

NASA CR/108502

11176-H546-RO-00

PROJECT TECHNICAL REPORT

TASK E-9G

# COMMUNICATIONS STUDY FOR THE PARTICLES AND FIELDS LUNAR SUBSATELLITE

NAS 9-8166

21 May 1970

Prepared for

NATIONAL AERONAUTICS AND SPACE ADMINISTRATION
MANNED SPACECRAFT CENTER
HOUSTON, TEXAS


Prepared by

L. A. Lorio


Approved by: J. G. Prothro

J. G. Prothro, Manager
Task E-9G

Approved by: John DeVillier

John DeVillier, Manager
Communication and Sensor
Systems Department

TRW
SYSTEMS GROUP

PRECEDING PAGE BLANK NOT FILMED.

CONTENTS

PRECEDING PAGE BLANK NOT FILMED.

TABLES

PRECEDING PAGE BLANK NOT FILMED.

ILLUSTRATIONS

## 1.0 INTRODUCTION AND SUMMARY

Presented herein is a brief study of TRW's proposed downlink communications system for the Particles and Fields Lunar Subsatellite. In the original proposal, Reference 1, a 3.9 kHz square-wave subcarrier was to be frequency-shift keyed at a 100 bps rate and then phase modulated onto a 2282.5 MHz carrier. A standard IRIG frequency discriminator in an 85-foot MSFN receiver was to demodulate the subcarrier.

Below are listed the results of this study for the above modulation scheme with either a square-wave or a sine-wave subcarrier.

1. Frequency components which are of the order of magnitude of the carrier and contained in a band whose center frequency is 3.9 kHz away from the carrier frequency could affect carrier acquisition since these components are within the sweepwidth used in acquiring the carrier. A possible solution to this problem is to acquire an unmodulated carrier before turning on the modulation.

2. For a sine-wave subcarrier at $\beta = 1.84$, 77.75% of the total power is contained in the carrier and the spectrum about the first sideband pair. For $\beta = 1.6$ this figure is 85.7%. For a square-wave subcarrier, this figure is 86.6% for $\beta = 1.0$ and 84.0% for $\beta = 1.16$. $\beta$ is the modulation index for the subcarrier onto the carrier.

3. For nominal values of parameters (see Table 3-1) with various values of $\beta$, the calculated RF margins for the carrier channel ranged from +6.9 to +11.6 dB and the margins for the information channel ranged from +7.3 to +8.3 dB. Using worst case system parameters, the carrier-channel margins ranged from -3.4 to +4.1 dB and the information-channel margins varied from +0.5 to +1.7 dB. Limiter effects could degrade the above margins by as much as 1 dB. There is no significant difference in these margins between the

sine-wave and square-wave subcarrier cases provided $\beta$ is appropriately chosen.

4. The relative power distribution in the predetection bandwidth is the same whether a sine-wave or a square-wave subcarrier is used.

5. Continuous phase at the frequency jumps of the subcarrier oscillator causes the predetection power spectrum to be concentrated near the two separate oscillator frequencies. For discontinuous phase the bandwidth of the power spectrum is larger.

6. For a 50 Hz square-wave data signal and subcarrier mark and space frequencies of 3.7 kHz and 4.1 kHz, only 2% of the signal power lies outside an ideal filter of 655 Hz bandwidth centered at 3.9 kHz. Continuous oscillator phase is assumed. Discontinuous phase causes a larger power loss.

7. The standard IRIG filter is 1 to 2 dB down at 3.7 kHz and 4.1 kHz. This could cause some loss in signal power.

In a later agreement, Reference 2, between MSC/GSFC/TRW, a 32.768 kHz square-wave subcarrier is to be biphase modulated with 128 bps data. (The modulation will be IRIG NRZ-M format). The subcarrier will then be phase modulated onto the 2282.5 MHz carrier. This technique will require installing biphase demodulators at the MSFN stations compatable with the subcarrier frequency.

Results 2 and 4 above apply equally well to this biphase modulation technique. The carrier-channel margins of Result 3 are applicable and the phase-shift keying method is expected to provide information-channel margins approximately 4 dB better than for the frequency-shift keying technique for the same system parameters. In the near future NASA/MSC will test carrier acquisition (see Result 1 above) when a 32.8 kHz subcarrier is used.

## 2.0 MODULATION LOSSES

### 2.1 SINE-WAVE SUBCARRIER

Although use of a square-wave subcarrier is planned, the modulation losses for a sine-wave subcarrier are given in this subsection for comparison. These results apply to either a frequency-shift keyed (FSK) or a biphase modulated subcarrier.

The expression for an angle modulated sinusoidal subcarrier which is phase modulated onto the S-band carrier is

$$e_1(t) = A \sin\left\{\omega_c t + \beta \sin\left[\omega_o t + \theta(t)\right]\right\} \tag{2-1}$$

where A is an amplitude constant, t is time (seconds), and $\beta$ is the phase modulation index (radians). The subcarrier and carrier radian frequencies are respectively $\omega_o$ and $\omega_c$. For the biphase modulated case $\theta(t)$, an arbitrary phase function at this point, will be equal to either 0 or $\pi$ radians in accordance with the state of the random code. In the FSK case, the value of the time derivative of $\theta(t)$ will equal either $+\omega_d$ or $-\omega_d$ according to the state of the random code. The radian frequency shift of the subcarrier will thus be $\pm\omega_d$.

Using the identity

$$\exp(j\beta \sin\phi) = \sum_{n=-\infty}^{\infty} J_n(\beta)\exp(jn\phi) \tag{2-2}$$

Equation (2-1) can be written as

$$e_1(t) = A\sum_{n=-\infty}^{\infty} J_n(\beta)\sin\left[(\omega_c + n\omega_o)t + n\theta(t)\right] \tag{2-3}$$

Assuming a 1 ohm load, the total power of $e_1(t)$ is

$$P_t = \frac{A^2}{2} \tag{2-4}$$

For n = 0 in Equation (2-3), the power in the carrier component of $e_1(t)$ is

$$P_c = \frac{A^2}{2} J_0^2(\beta) \tag{2-5}$$

Defining the carrier modulation loss, $L_c$, from

$$P_c = L_c P_t \tag{2-6}$$

gives $$L_c = J_0^2(\beta) \tag{2-7}$$

The ground station beats $e_1(t)$ down in frequency so that the spectrum of Equation (2-3) becomes centered about 0 Hz rather than the carrier frequency. The subcarrier predetection bandpass filter (assumed ideal) centered about $\omega_0$ passes the n = ±1 components of Equation (2-3). Hence, the power in the filter bandwidth is

$$P_d = A^2 J_1^2(\beta) \tag{2-8}$$

Defining the data modulation loss, $L_d$, from

$$P_d = L_d P_t \tag{2-9}$$

gives

$$L_d = 2 J_1^2(\beta) \tag{2-10}$$

## 2.2 SQUARE-WAVE SUBCARRIER

Let f(t) be a square-wave subcarrier of unity amplitude which is either frequency-shift keyed or biphase modulated. In either case f(t) takes on only values of +1 or -1. The expression for f(t) phase modulated onto the carrier is

$$e_2(t) = A \sin\left[\omega_c t + \beta f(t)\right] \tag{2-11}$$

Upon expanding

$$e_2\ (t) = A \sin\ (\omega_c t) \cos \left[ \beta f(t) \right]$$
$$+ A \sin\ [\beta f(t)] \cos\ (\omega_c t) \qquad (2\text{-}12)$$

Since $\cos\ (\beta) = \cos\ (-\beta)$, then $\cos \left| \beta f(t) \right| = \cos \beta$. Since $\sin\ (-\beta) = -\sin\ (\beta)$, then $\sin \left| \beta f(t) \right| = f(t) \sin\ (\beta)$. Therefore,

$$e_2\ (t) = A \cos\ (\beta) \sin\ (\omega_c t) + A\ f(t) \sin\ (\beta) \cos\ (\omega_c t) \qquad (2\text{-}13)$$

The first term is the carrier component and the second term is an amplitude modulated signal with the carrier suppressed.

Let g(t) represent a square wave whose amplitude changes from -1 to +1 at $t = \tau$. Then

$$g(t) = \frac{4}{\pi} \sum_{\substack{n = 1,3 \\ \text{odd}}}^{\infty} \frac{1}{n} \sin \left[ n\omega_1 t - n\tau \right] \qquad (2\text{-}14)$$

where $\omega_1$ is the radian frequency of g(t). Notice that the fundamental component ($n = 1$) is in phase with the square wave. Now suppose that the FSK or biphase modulated subcarrier of Equation (2-1) is the fundamental component of g(t). Hence,

$$f(t) = \frac{4}{\pi} \sum_{\substack{n = 1,3 \\ \text{odd}}}^{\infty} \frac{1}{n} \sin \left[ n\omega_o t + n\theta(t) \right] \qquad (2\text{-}15)$$

Then

$$e_2(t) = A \cos\ (\beta) \sin\ (\omega_c t)$$
$$+ \frac{4A}{\pi} \sin\ (\beta) \cos\ (\omega_c t) \sum_{\substack{n = 1,3 \\ \text{odd}}}^{\infty} \frac{1}{n} \sin\ [n\omega_o t + n\theta(t)] \qquad (2\text{-}16)$$

$$e_2(t) = A \cos\ (\beta) \sin\ (\omega_c t)$$
$$+ \frac{2A}{\pi} \sin\ (\beta) \sum_{\substack{n = -\infty \\ \text{odd}}}^{\infty} \frac{1}{n} \sin\ [(\omega_c + n\omega_o)t + n\theta(t)] \qquad (2\text{-}17)$$

The carrier modulation loss (see Equation 2-6) is

$$L_c = \cos^2(\beta) \tag{2-18}$$

The data modulation loss (see Equation 2-9) is

$$L_d = \frac{8}{\pi^2}\sin^2(\beta) \tag{2-19}$$

$L_c$ and $L_d$ for a sine-wave and a square-wave subcarrier are plotted in Figure 2-1 as a function of $\beta$.

A comparison of Equations (2-3) and (2-17) indicates that the relative power distribution within the predetection bandwidth ($n = \pm 1$ terms) is the same whether a sine-wave or a square-wave subcarrier is used. Of course, the total amount of power in this bandwidth is proportional to the data modulation loss, $L_d$.

## 2.3 DISCUSSION OF MODULATION LOSSES

For the sine-wave subcarrier at $\beta = 1.6$, $L_c = -6.8$ dB and $L_d = -1.9$ dB. $L_d$ attains its maximum value of -1.7 dB if $\beta$ is increased to 1.84, but $L_c$ is degraded by 3.2 dB.

For the square-wave subcarrier at $\beta = 1.1$, $L_c = -6.9$ dB and $L_d = -1.9$ dB. These values are practically the same as for the sine-wave subcarrier above. For the square-wave subcarrier, $L_d$ could be improved slightly at the expense of $L_c$ by increasing $\beta$. However, for $\beta > 1.2$, the slope of the $L_c$ curve is rather steep. Hence, circuit misadjustments giving approximately a 10% higher $\beta$ than desired would cause a 3 dB or more degradation in $L_c$. $\beta = 1.0$ to 1.15 would be a good modulation index for the square-wave subcarrier.

For appropriate $\beta$, Table 2-1 shows approximately 85% of the total power of $e_1(t)$ or $e_2(t)$ in the carrier and $n = \pm 1$ components. Figures 2-2 through 2-5 are power spectral density plots of $e_1(t)$ and $e_2(t)$ for representative values of $\beta$ with $\theta(t) = 0$, i.e. the subcarrier is unmodulated.

For $\theta(t) \neq 0$, the power contained at each frequency indicated in these figures will be spread out into a narrow frequency band centered at the frequencies where the lines appear. Observe that the power spectrum falls off at a much slower rate for increasing n for a square-wave subcarrier than for a sine-wave subcarrier.

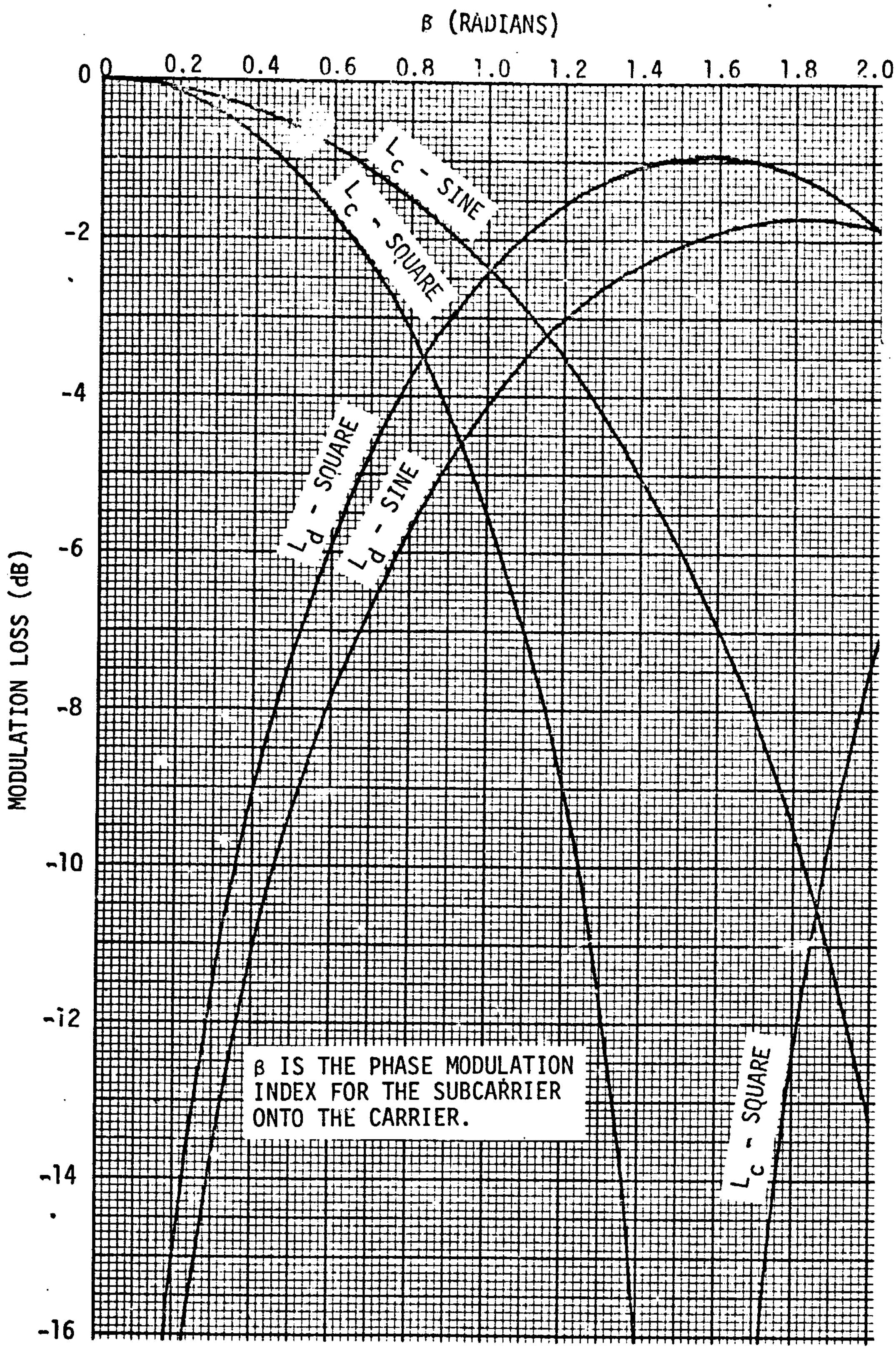


Figure 2-1. Modulation Losses for Sine-Wave and Square-Wave Subcarriers

Table 2-1. Percentage of Total Power in the nth Sideband Pair[a]

| n | Sine-Wave Subcarrier | | Square-Wave Subcarrier | |
|---|---|---|---|---|
| | $\beta$ = 1.6 | $\beta$ = 1.84 | $\beta$ = 1.0 | $\beta$ = 1.16 |
| 0 | 20.70 | 10.03 | 29.19 | 15.94 |
| 1 | 64.98 | 67.72 | 57.40 | 68.10 |
| 2 | 13.21 | 19.94 | | |
| 3 | 1.07 | 2.19 | 6.37 | 7.57 |
| 4 | 0.04 | 0.13 | | |
| 5 | | <0.01 | 2.30 | 2.73 |
| 6 | | | | |
| 7 | | | 1.17 | 1.39 |
| 8 | | | | |
| 9 | | | 0.71 | 0.84 |

(a) Radian frequencies of the sidebands are $(\omega_c + n\,\omega_1)$ and $(\omega_c - n\,\omega_1)$ where $\omega_c$ and $\omega_1$ are the carrier and subcarrier frequencies respectively.

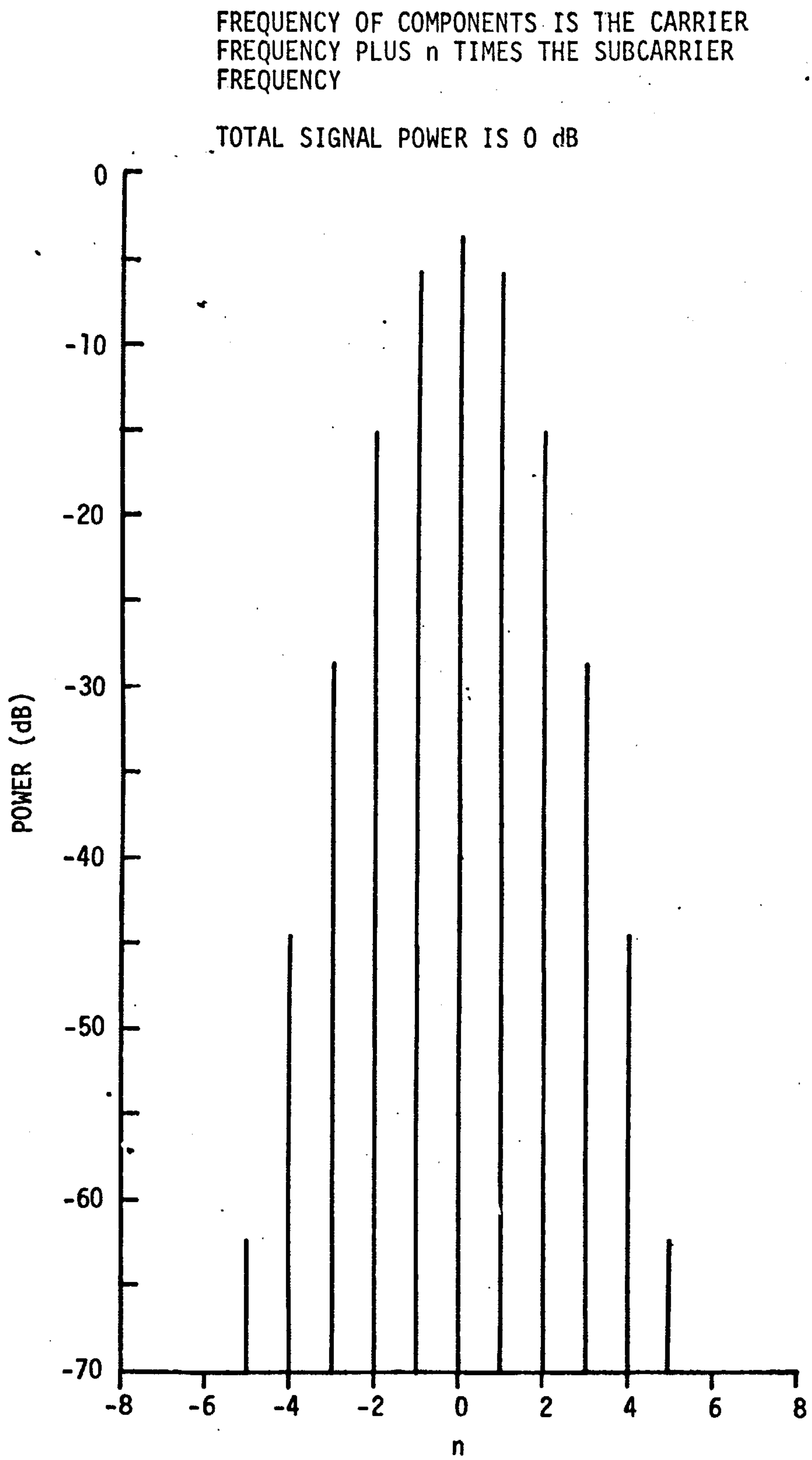


Figure 2-2. Spectrum About the Carrier for an Unmodulated Sine-Wave Subcarrier ($\beta$ = 1.25)

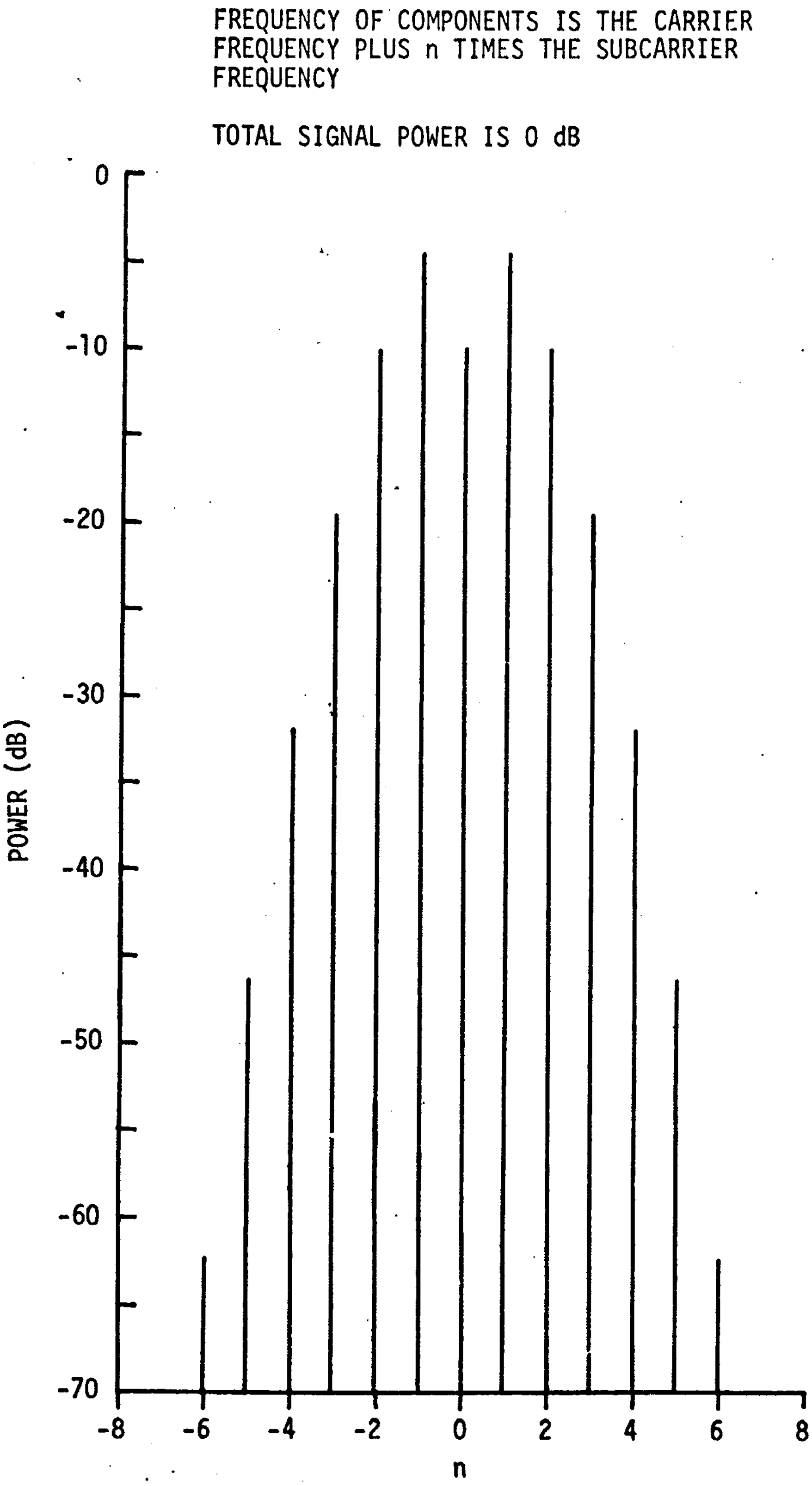


Figure 2-3. Spectrum About the Carrier for an Unmodulated Sine-Wave Subcarrier ($\beta = 1.84$)

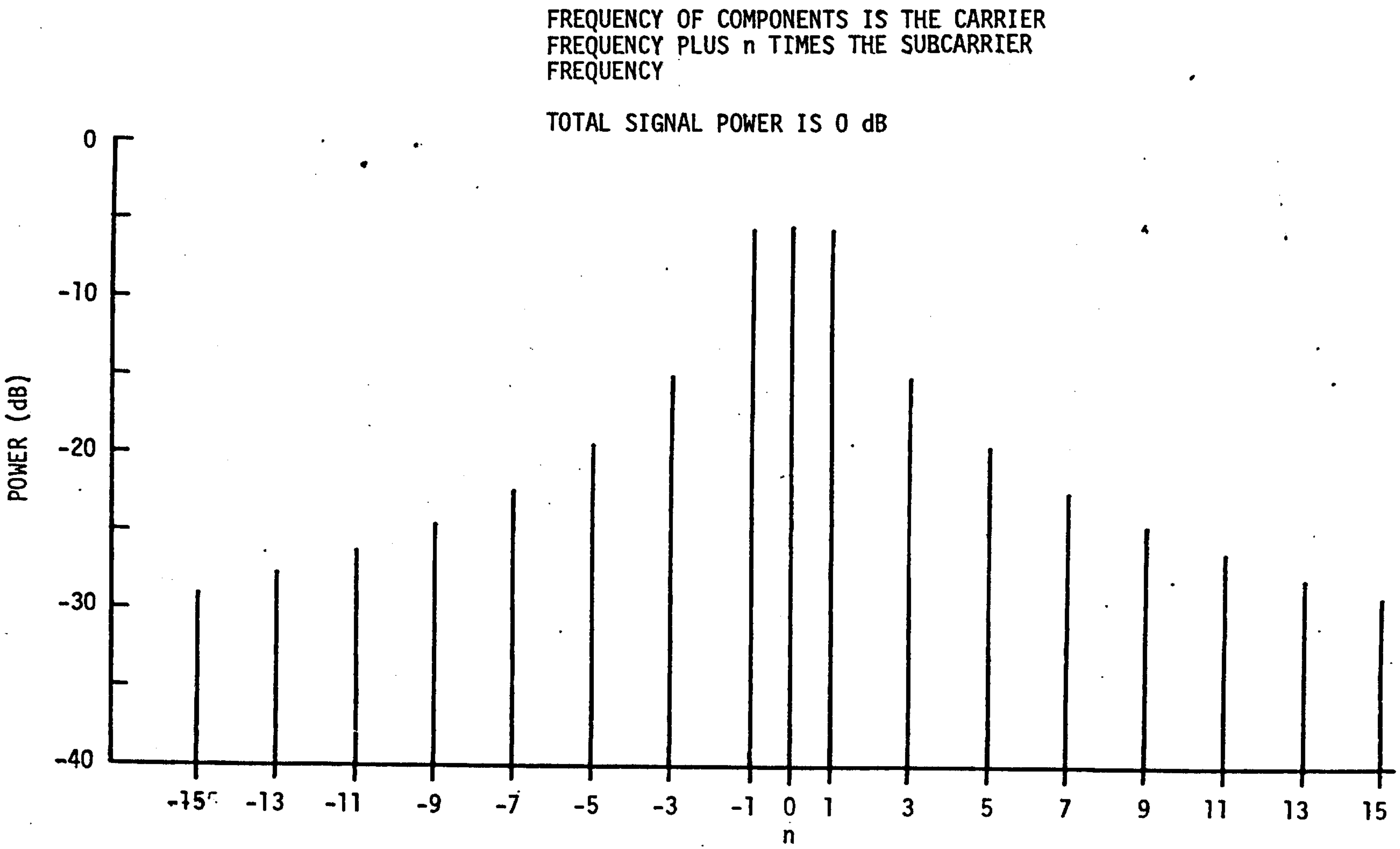


Figure 2-4. Spectrum About the Carrier for an Unmodulated Square-Wave Subcarrier ($\beta = 1.0$)

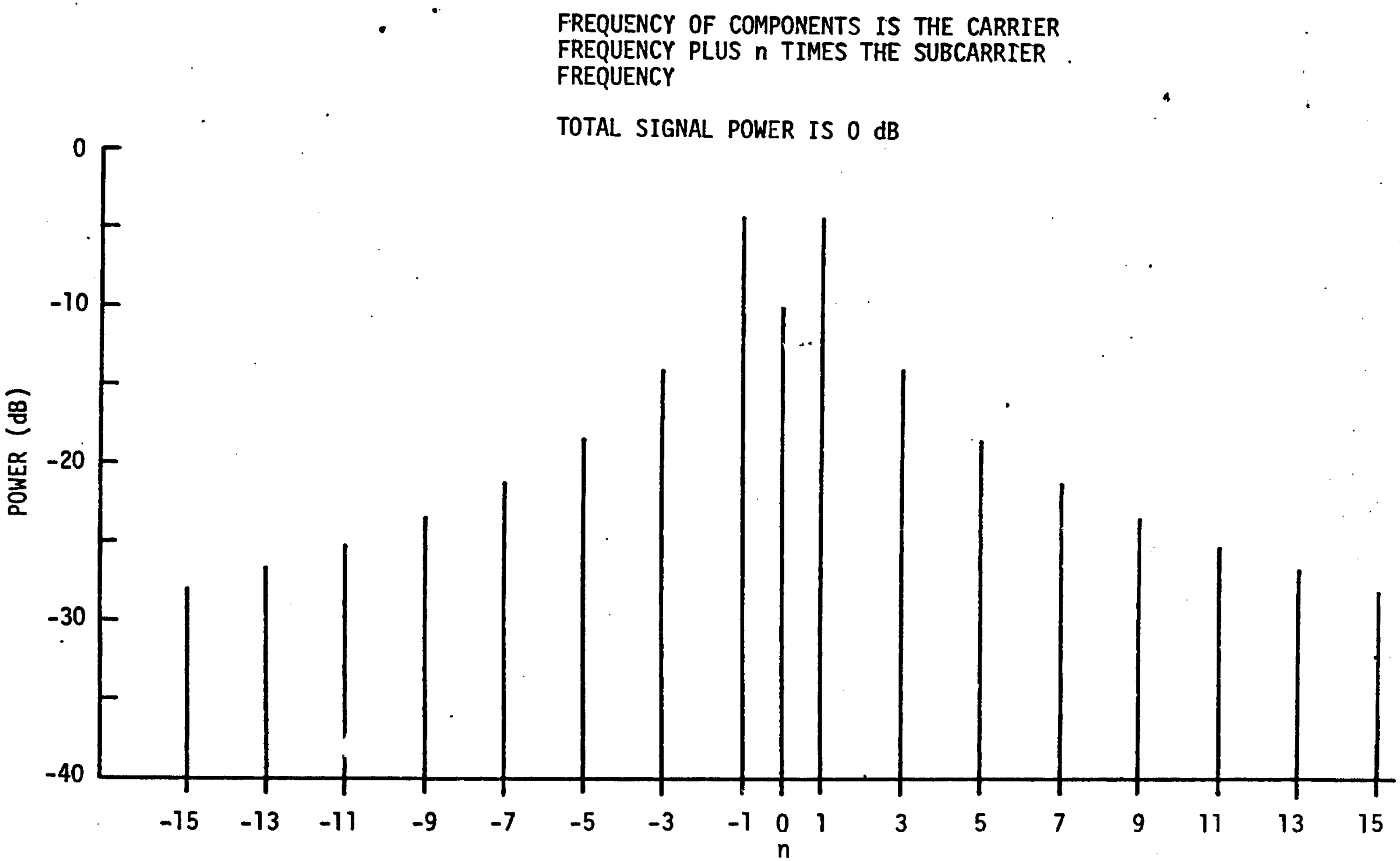


Figure 2-5. Spectrum About the Carrier for an Unmodulated Square-Wave Subcarrier ($\beta = 1.25$)

## 3.0 MARGIN CALCULATIONS

RF margins were calculated for the downlink communications system which was to use a frequency-shift-keyed, 3.9 kHz subcarrier.

A frequency discriminator in the receiver of an 85-foot MSFN station was to be used to recover the data. A standard IRIG bandpass filter was to feed the part of the baseband signal centered about 3.9 kHz ($n = \pm 1$, $\omega_c = 0$ in Equations (2-3) and (2-17)) to the discriminator input. An ideal IRIG filter was assumed for margin calculations.

For margin calculations, the S-band math model for the Apollo PM communications system (Reference 3) was used along with the parameters in Table 3-1. The calculated margins are shown in Tables 3-2 and 3-3. Limiter effects have not been included and could degrade these margins by as much as 1 dB.

Nominal parameter values yield adequate circuit margins which are approximately the same for the sine-wave and square-wave subcarrier cases. However, with worst case parameters either system is marginal.

For biphase modulation of a 32.8 kHz subcarrier the information-channel margins in Table 3-3 are expected to improve by 4.2 dB. This is based on a change in the required predetection SNR from 8.0 dB (Table 3-1) to 3.8 dB (Reference 3) for low bit rate telemetry with a bit error probability of $10^{-4}$. Also, this assumes that the values of the other parameters of Table 3-1 remain the same.

Table 3-1. Parameters Used to Calculate RF Margins

| Quantity | Nominal Value | Worst Case | Reference |
|---|---|---|---|
| Carrier frequency | 2282.5 MHz | 2282.5 MHz | 1 |
| Transmitted Power | 29.0 dBm | 27.0 dBm | 1 |
| Transmit antenna gain | +1 dB | -2 dB | 1 |
| Range | 215,000 n.mi. | 215,000 n.mi. | |
| Polarization loss | 0 dB | -0.2 dB | 1 |
| 85-foot MSFN receive antenna gain | 53.0 dB | 52.5 dB | 3 |
| Diplexer, cable, and misc. losses | -0.9 dB | -1.0 dB | 1 |
| Carrier channel noise bandwidth | 50 Hz | 50 Hz | 3 |
| Information channel noise bandwidth | 655 Hz | 720 Hz | 3 |
| Modulation index, $\beta$ | | ±10% change | |
| (SNR) required for carrier channel | 12 dB | 12 dB | 3 |
| (SNR) required at discriminator input | 8 dB[(a)] | 8 dB | |
| Noise spectral density constant for 85-foot antenna | $210^{o}K$ | $210^{o}K$ | 3 |

(a) From recent tests conducted at NASA/MSC for $10^{-4}$ BEP.

Table 3-2. Carrier RF Margins

| Subcarrier Type | Nominal $\beta$ | $L_c$ (dB) Nominal | Carrier Channel Margins (dB) Nominal | Worst Case |
|---|---|---|---|---|
| Sine | 1.6 | - 6.8 | +10.1 | +2.3 |
| Sine | 1.84 | -10.0 | + 6.9 | -1.9 |
| Square | 1.0 | - 5.3 | +11.6 | +4.1 |
| Square | 1.16 | - 8.0 | + 8.9 | +0.2 |
| Square | 1.25 | -10.0 | + 6.9 | -3.4 |

Table 3-3. Information-Channel RF Margins

| Subcarrier Type | Nominal $\beta$ | $L_d$ (dB) Nominal | Information-Channel RF Margins (dB) Nominal | Worst Case |
|---|---|---|---|---|
| Sine | 1.6 | - 1.9 | +7.8 | +1.3 |
| Sine | 1.84 | - 1.7 | +8.0 | +1.7 dB |
| Square | 1.0 | - 2.4 | +7.3 | +0.5 dB |
| Square | 1.16 | - 1.7 | +8.0 | +1.3 dB |
| Square | 1.25 | - 1.4 | +8.3 | +1.6 dB |

# 4.0 PREDETECTION SIGNAL SPECTRUM

## 4.1 FREQUENCY-SHIFT-KEYED SUBCARRIER

The baseband signal at the input to the predetection filter is $e_1(t)$ when $\omega_c=0$ (Equation (2-3)) for the sine-wave subcarrier or $e_2(t)$ when $\omega_c=0$ (Equation (2-17)) for the square-wave subcarrier. For either modulation technique (FSK or biphase) the $n = \pm 1$ terms of these equations contribute the signal, s(t), within the filter passband. For K a constant, s(t) is of the form

$$s(t) = \frac{1}{2} K \sin [\omega_o t + \theta(t)] - \frac{1}{2} K \sin [-\omega_o t - \theta(t) \tag{4-1}$$

$$= K \sin [\omega_o t + \theta(t)] \tag{4-2}$$

For the FSK case, the subcarrier radian frequency will be either $(\omega_o + \omega_d)$ or $(\omega_o - \omega_d)$ in accordance with the state of the random code. Hence, the time derivative of $\theta(t)$ will be either $+\omega_d$ or $-\omega_d$ (except at the transition times when the derivative is not defined). Let T equal the length of 1 bit in seconds and define k from

$$\pi k = \omega_d T \tag{4-3}$$

For k an integer, an integral number of cycles of either subcarrier frequency occurs in time T.

Assume the bit stream is a square wave of period 2T. If $\theta(t)$ is a continuous function (no phase discontinuities at the times of frequency transitions), Reference 4 gives the Fourier series expansion

$$s(t) = K \sum_{n=-\infty}^{\infty} c_n \sin [\omega_o t + \frac{n\pi t}{T}] \tag{4-4}$$

where

$$c_n = \frac{2k \sin [(k + n) \pi/2]}{\pi (k^2 - n^2)} \tag{4-5}$$

If k is an integer, then $c_n = 1/2$ when $n = \pm k$ and 50% of the power in s(t) is in the components at $(\omega_o + \omega_d)$ and $(\omega_o - \omega_d)$. If k is an even integer, then $c_n = 0$ for n even and not equal to $\pm k$.

Assume an ideal predetection filter centered at 3.9 kHz = $\omega_o/2\pi$ with a bandwidth of 655 Hz. For $\omega_d/2\pi$ = 300 Hz and a 50 Hz square-wave bit stream (100 bps) k = 6. Therefore, the filter passes frequency components through n = 6 or 80.5% of the power in s(t), the input.

If k is changed to 4 by choosing $\omega_d/2\pi$ = 200 Hz, then only 1.7% of the power in s(t) lies outside the filter passband. Figure 4-1, the power density spectrum, shows a concentration of power about the mark and space frequencies of 3.7 kHz and 4.1 kHz. Since the response of an actual IRIG predetection filter is 1 to 2 dB down at these frequencies, some signal power would be lost.

If the phase function, $\theta(t)$, is not continuous at the times of frequency changes, the spectrum of s(t) depends on the type of phase discontinuities. If s(t) is formed by alternately switching at the bit rate between two independent oscillators set at the mark and space frequencies, Reference 4 gives the associated amplitude spectrum. For this case the power in the high order sidebands falls off as $n^{-2}$ (for the nth sideband). By comparison, for continuous phase, the power in the higher order sidebands falls off as $n^{-4}$, i.e. more rapidly.

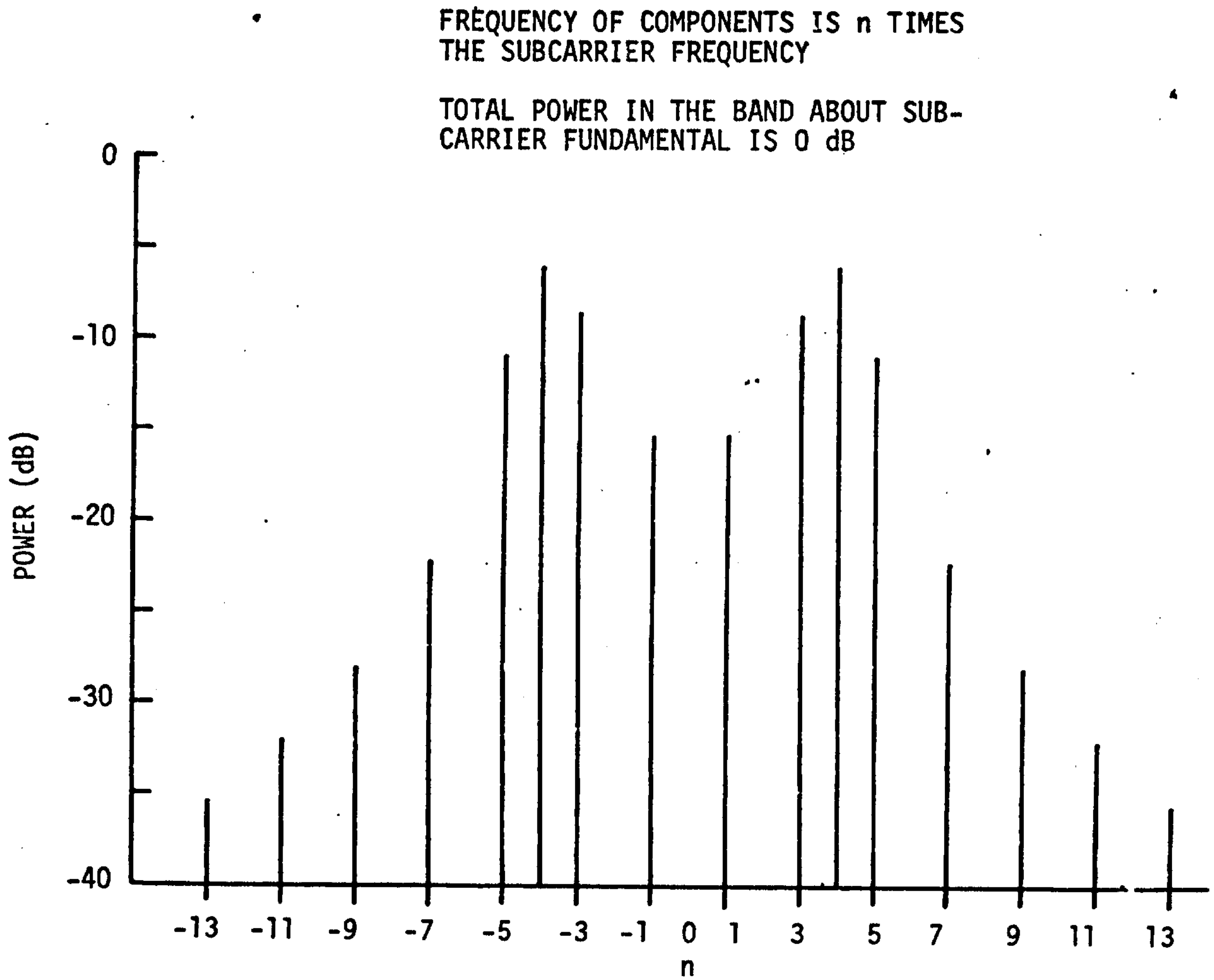


Figure 4-1. Spectrum About the Subcarrier Fundamental for a Frequency-Shift-Keying, Square-Wave, Modulating Signal (k=4)

## 4.2 BIPHASE MODULATED SUBCARRIER

The expression for the signal within the passband of the predetection filter when either a sine-wave or square-wave subcarrier is biphase modulated is given by Equation (4-2) when $\theta(t)$ takes the values of 0 or $\pi$ in accordance with the state of the random code. If $m(t) = +1$ when $\theta(t) = 0$ and $m(t) = -1$ when $\theta(t) = \pi$, then

$$s(t) = K\, m(t) \sin (\omega_0 t) \tag{4-6}$$

Let T be the length of 1 bit in seconds. If the bit stream is a square wave of period 2T and frequency $f_1$ Hz then

$$s(t) = \frac{4K}{\pi} \sin (\omega_0 t) \sum_{\substack{n=1,3 \\ \text{odd}}}^{\infty} \frac{1}{n} \sin (2n\pi f_1 t) \tag{4-7}$$

For 128 bps data, $f_1 = 64$ Hz. The power in either the component at $(\omega_0 + n\omega_1)$ or $(\omega_0 - n\omega_1)$ is $2K^2/n^2\pi^2$ for odd n. Figure 4-2 shows the power spectrum with the 0 dB reference taken as 1 watt = $K^2/2$ = the total power in s(t). In Reference 5, some amplitude spectrums are plotted for a subcarrier biphase modulated with various periodic codes.

Consider biphase modulation with a random code. Suppose probabilities are assigned to the occurence of $m(t) = +1$ and $m(t) = -1$ and let the value of m(t) in each bit interval be independent of the values of m(t) in all other intervals. Then the expression for the power density function averaged over the ensemble of all possible codes is derived in Reference 4. When each value of m(t) is equally likely, the average power density function (Reference 5) is

$$W(\omega) = \frac{2K^2 \sin^2 [(\omega-\omega_0)\, T/2]}{T\, (\omega-\omega_0)^2} \tag{4-8}$$

$W(\omega)$ can be compared with Figure 4-2. If $\omega = \omega_0 \pm n\pi/T$ with n an integer, then $W(\omega) = 0$ for even, non-zero n (as in Figure 4-2) and for n odd, $W(\omega) = 2K^2T/n^2\pi^2$. Except for n=1, $W(\omega)$ attains approximately its peak values when n is odd. At n=0, $W(\omega)$ has its maximum value of $K^2T/2$. Observe that the value of $W(\omega)$ for each odd n is T times the power in the line at $(\omega_0 + n\omega_1)$ or $(\omega_0 - n\omega_1)$ in Figure 4-2. For the proposed bit rate of 128 bps, the peaks of $W(\omega)$ would be approximately 21.07 dB (10 log T = -21.07 dB) lower than the lines indicated in Figure 4-2.

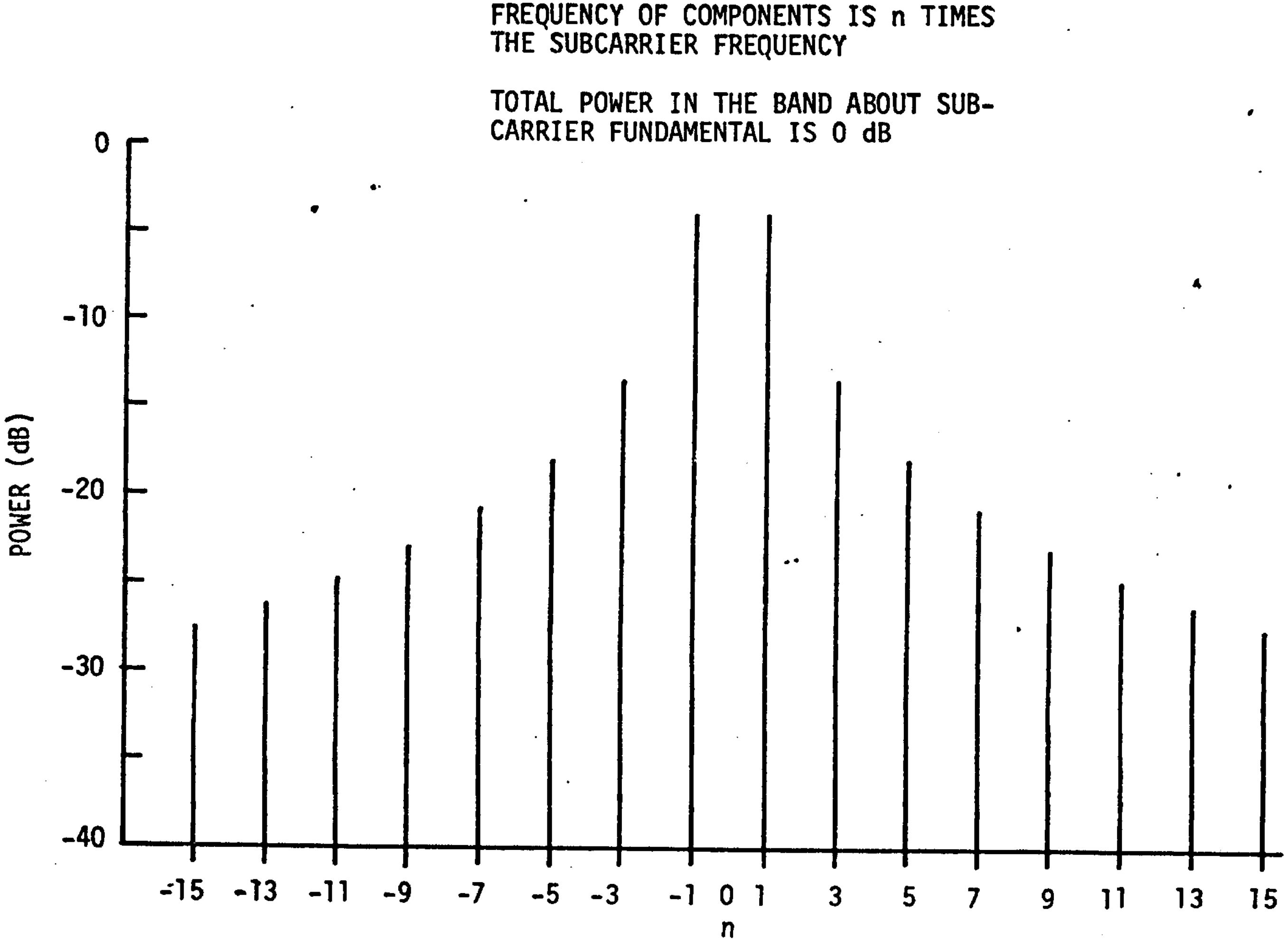


Figure 4-2. Spectrum About the Subcarrier Fundamental for a Biphase - Modulating, Square-Wave, Modulating Signal

## 5.0 CARRIER ACQUISITION

From Section 4, there are frequency components of the order of magnitude of the carrier in a band centered at 3.9 kHz (subcarrier frequency) away from the carrier frequency. Since these components are within the sweepwidth used in acquiring the carrier in the carrier tracking loop, it is possible to lock on to them rather than the S-band carrier (i.e. false carrier lock). In the past, telemetry spurs which were 51.2 kHz away from the carrier frequency and 20 to 30 dB below the carrier level have caused false carrier locks when they were within the sweep range of the carrier loop. This problem could possibly be avoided either by acquiring the downlink carrier prior to modulating it or by making the subcarrier frequency greater than the sweepwidth of the carrier loop.

Acquisition problems could exist if the sweepwidth were made less than ±12 kHz which was the typical shift in carrier frequency resulting from doppler effects for the CSM in lunar orbit on the Apollo 11 and 12 missions. For the FSK case, an IRIG subcarrier of frequency higher than 3.9 kHz would result in negative RF margins in the data channel under worst case parameter values because of the larger noise bandwidth of the associated IRIG predetection filter. Hopefully, when a biphase-modulated, 32.768 kHz subcarrier is used, the carrier can be satisfactorily acquired. Carrier acquisition tests will be conducted at NASA/MSC to determine if this is the case. For the parameter values of Table 3-1, biphase modulation yields positive RF margins (see Section 3).

## REFERENCES


1. "Proposal for a Particles and Fields Subsatellite for the Apollo Lunar Program," TRW Proposal 16763.000, March 1970.

2. J. H. Johnson, "Subsatellite Communications," NASA/MSC Memorandum, EE17/70-44, 10 April 1970.

3. "Communication Systems Performance and Coverage Analysis for Apollo 13 (H-2 Mission), Volume 1, Operational Data," MSC Internal Note MSC-01831, TRW 11176-H483-R0-00, 27 February 1970.

4. W. R. Bennett and J. R. Davey," Data Transmission," McGraw-Hill Book Company, New York, 1965, pp. 38-48, 315-333.

5. R. J. Panneton, "Analysis of Reduction in the 1.024 MHz Telemetry Subcarrier Modulation Index," TRW 11176-H023-R0-00, 21 August 1968.